

## Structural study of silica particle dispersions by ultra-small-angle x-ray scattering

Toshiki Konishi and Norio Ise\*

*Fukui Research Laboratory, Rengo Co., Ltd. Jiyūgaoka, Kanazu-cho, Sakai-gun, Fukui 919-06, Japan*

Hideki Matsuoka and Hitoshi Yamaoka

*Department of Polymer Chemistry, Kyoto University, Kyoto 606-01, Japan*

Ikuo S. Sogami and Tsuyoshi Yoshiyama

*Department of Physics, Kyoto Sangyo University, Kyoto 603, Japan*

(Received 10 August 1994)

An ultra-small-angle x-ray-scattering study showed several orders of Bragg diffraction for an aqueous colloidal silica dispersion in a vertically held glass capillary, the first peak being at  $150''$ . The same profile was observed when the capillary was rotated around its axis by  $(60 \times m)^\circ$  (where  $m$  is an integer). A different profile was found at  $(30 + 60 \times m)^\circ$  with the first peak at  $85''$ . This showed that a bcc lattice was maintained with the (110) plane parallel to the capillary wall and with a lattice constant  $= 3000 \text{ \AA}$ ,  $d_{110} = 2100 \text{ \AA}$ , and  $d_{020} = 1500 \text{ \AA}$ . The closest interparticle distance ( $2D_{\text{exp}}$ ) was  $2600 \text{ \AA}$  while the average distance from the overall concentration ( $2D_0$ ) was  $2900 \text{ \AA}$ , indicating the non-space-filling nature of the crystal.

It is well known that monodisperse, ionic colloidal particles form an ordered structure in dispersions.<sup>1</sup> Various techniques have been employed to clarify the fundamental aspects of the structure formation. For example, microscopic studies provide the most straightforward information, but this is local rather than global information.<sup>2</sup> Intrinsic Kossel line analysis has been demonstrated to be highly reliable in structural studies of colloidal crystals because of a one-to-one correspondence between the Kossel pattern and the crystal symmetry.<sup>3</sup> Scattering methods (neutron and light), though frequently used, have usually provided only one or two broad diffraction peaks, so that the structural parameters could not be precisely determined. These studies have shown that the lattice constant of colloidal crystals, or the interparticle distance, is of the order of 0.1 to  $1 \mu\text{m}$ , which is much larger than that of atomic or molecular crystals. Though the latter crystals have been studied accurately by x-ray diffraction, this technique could not be employed for colloidal systems because density fluctuations of such a large scale have been out of the reach of conventional x-ray diffractometers. Recently an ultra-small-angle x-ray-scattering (USAXS) apparatus<sup>4</sup> has been constructed using the principle of Bonse and Hart.<sup>5</sup> This enabled us to detect scattered x rays at very low angles (down to 4 sec of arc) with high resolution. The USAXS method has been applied to various systems including colloidal dispersions.<sup>4,6,7</sup> For example, dispersions of latex particles showed powderlike patterns characteristic of face-centered-cubic (fcc) systems, from which the interparticle distance could be estimated.<sup>4,7</sup> In the present report, we described an USAXS apparatus, which was applied to the study of an aqueous dispersion of silica particles. In this paper several orders of Bragg diffraction (up to five) have been reported for a colloidal crystal. Thus we could determine the lattice system and lattice constant more precisely than in previous scattering experiments.

The colloidal silica dispersion used in this work was KE-P10W, kindly donated by Nippon Shokubai Co., Ltd., Osaka, Japan. The z-average radius  $R$  of the particles and its standard deviation were  $560 \text{ \AA}$  and 8%, respectively, which were obtained by fitting observed USAXS profiles under high salt conditions to the form factors for isolated spheres. The net charge density of the particles was  $0.06 \mu\text{C}/\text{cm}^2$  by conductometric measurements, with the analytical charge density being  $0.24 \mu\text{C}/\text{cm}^2$ . The original dispersion in water (20 wt. %) was dialyzed against Milli-Q reagent grade water for purification. After dilution with Milli-Q water, the concentration of silica was determined to be 3.76 vol. % by dry weight using  $2.2 \text{ g}/\text{cm}^3$  for its specific gravity. The dispersion was introduced into a glass capillary (length: 70 mm) of an inner diameter of 2 mm together with ion-exchange resin particles [AG501-X8 (D), Bio-Rad Lab., Richmond, CA]. The upper part of the capillary (separated by a nylon mesh) and the lower part were filled with the resin particles. The middle part, where the x-ray beam (width: about 1 mm, height: about 15 mm) hits, was free from the resin particles. The dispersion inside the capillary was iridescent.

The USAXS apparatus used in this work was constructed in Fukui Research Laboratory, Rengo Co., Ltd., by Rigaku Corporation, Tokyo. It is composed of an x-ray generator, Rotaflex RU-300 (60 kV–300 mA, target:Cu) and a Bonse-Hart camera (with Si or Ge single crystals). It is an improved version of that previously constructed.<sup>4</sup> The top view of the present camera (with Si crystals) is shown in Fig. 1. In the present experiments, the Ge crystals were used in order to utilize x-rays of higher intensities. In this system, two grooved Ge single crystals, which are cut along the direction parallel to the (220) plane of the crystals, are used instead of slits. In the groove of the first (Ge) crystal, the x-ray beam is Bragg reflected four times, including an asymmetric

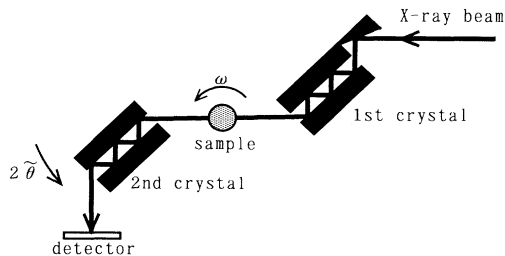


FIG. 1. The optical system of the USAXS apparatus with Si single crystals. The principle was the same for the Si and Ge crystals except that the number of reflections in both the first and second crystals were 5 and 3, for Si and Ge, respectively. The angle  $2\bar{\theta}$  is the rotation angle of the second crystal with respect to a vertical axis. The zero angle of the  $2\bar{\theta}$  is defined as the position where the incident x-ray beam out of the first crystal (without sample) is reflected from the second crystal. (The angle  $2\bar{\theta}$  is not the true scattering angle  $2\theta$  but the angle between a vertical plane including the path of the incident x ray into the sample and that containing the path of the scattered x ray out of the sample.)

reflection, so that the incident x-ray beam out of the first crystal into the sample is highly monochromatic and parallel. The wavelength ( $\lambda$ ) of the x-ray beam is 1.540562 Å. In the groove of the second (Ge) crystal, only the part of the scattered x-ray beam that satisfies the Bragg condition repeats reflection three times, and can arrive at the detector. It should be noted that the individual incident or scattered x rays are highly parallel to each other only in the horizontal plane, but not in the vertical plane; in other words, this camera system can be regarded as being composed of infinitely long and thin slits. The small-angle resolution of the present apparatus is characterized by full widths at half maximum of the measured rocking curves of 11.1 and 4.0 sec of arc for the Ge and Si crystals, respectively. It is noted that the values of the full widths at half maximum are determined by the crystals but do not depend very much on the number of reflections which determine the steepness of the rocking-curve tails.

The scattering intensity  $I(2\bar{\theta})$  was measured with the second crystal rotated in the horizontal plane by  $2\bar{\theta}$  from the position where the incident beam (without sample) is reflected from the second crystal. Considering the optical system of the apparatus, which has a smearing effect in the vertical direction, the true diffraction angle  $2\theta$ , which is the angle made by the incident x ray in the horizontal plane with the scattered x ray, is equal to  $2\bar{\theta}/\cos\phi$ , where  $\phi$  is the angle made by the horizontal plane with the plane defined by the paths of the incident and the scattered x rays. The measurements were also performed by varying the rotation angle  $\omega$  of the sample with respect to the capillary axis, which was vertical.

In Fig. 2, the logarithm of the USAXS intensity is plotted against  $2\bar{\theta}$  for a silica particle dispersion in water. The capillary was kept standing vertically for 84 days after the dispersion was introduced into it. As seen in Fig. 2(a), sharp peaks were observed at diffraction angles of  $(150 \times n)''$ , with  $n$  being integer. These peaks correspond to Bragg reflections, where the diffraction angles

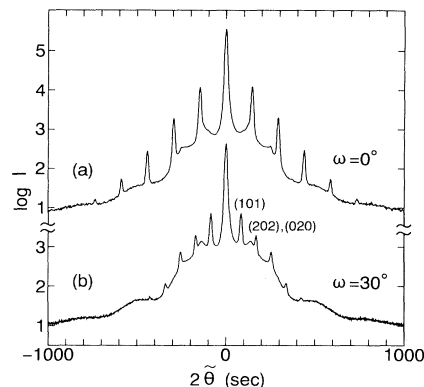


FIG. 2. The logarithm to base 10 of the USAXS intensity  $I(2\bar{\theta})$  in counts per second versus the rotation angle  $2\bar{\theta}$  of the second crystal. Sample: 3.76 vol. % water dispersion of silica particles (radius: 560 Å, standard deviation: 8%). Measurements were done 84 days after the dispersion was introduced into the capillary. Curve (a) rotation angle of the capillary  $\omega=0^\circ$ , curve (b)  $\omega=30^\circ$ . Temperature:  $25 \pm 1^\circ\text{C}$ .

are written as follows:

$$\sin\theta = n\lambda/2d, \quad (1)$$

with  $d$  being the distance between the diffraction planes. Since strong and sharp peaks with  $n$  up to five could be observed, it was considered that a very large single crystal of colloidal silica had grown in the capillary. We note that several orders of diffraction were also observed at each multiple angle of  $60 \pm 1^\circ$ , in other words, at  $\omega$  of  $(60 \times m) \pm 1^\circ$  with  $m$  being an integer, when the capillary tube was manually rotated around its axis. Furthermore, the dispersion in this capillary displayed similarly sharp peaks at diffraction angles of  $(85 \times n)''$  when the capillary was rotated by  $(30 + 60 \times m) \pm 1^\circ$  as shown in Fig. 2 (b).

From all the information, it was concluded that a body-centered-cubic (bcc) lattice was maintained in the capillary, with the  $[1\bar{1}1]$  direction of the single crystal being vertically upward and parallel to the capillary axis. The situation is represented in Figs. 3 and 4 for the cases  $\omega=0^\circ$  [corresponding to the USAXS curve shown in Fig. 2(a)] and  $\omega=30^\circ$  [Fig. 2(b)], respectively. Figure 3(a) shows a top view of the lattice points of the crystal in the capillary, while 3(b) is the side view from the direction parallel to the incident beam; the filled circles represent lattice points, i.e., the centers of the particles. The lattice planes that give rise to diffraction are denoted by solid lines with the corresponding Miller indices. It is noted that, from Fig. 3(a), exactly the same diffraction patterns may be expected for  $\omega=(60 \times m)^\circ$ . This is consistent with the fact that the same USAXS profile as shown in Fig. 2(a) appeared at these rotation angles. A similar situation arose when  $\omega$  is  $(30 + 60 \times m)^\circ$  which corresponds to Fig. 4, although the distribution of the lattice points becomes a mirror image in the case of  $\omega$  being  $(90 + 120 \times m)^\circ$ . This was also consistent with the experimental results. From Figs. 3 and 4, it was inferred that the profiles at  $\omega=(60 \times m)^\circ$  [Fig. 2(a)] correspond to the diffraction from the (110) planes. The first- and second-

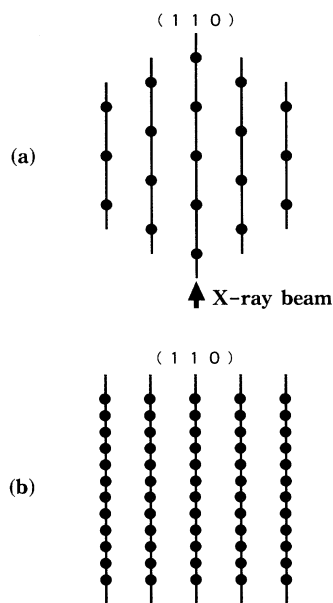


FIG. 3. A schematic illustration of the body-centered-cubic (bcc) lattice maintained in the capillary for the rotation angle of the capillary  $\omega=0^\circ$ , with the  $[\bar{1}\bar{1}1]$  direction of the lattice being vertically upward and parallel to the capillary axis. (a) a top view of the lattice points (filled circles). (b) a side view from the direction almost parallel to the incident x-ray beam [Fig. 2(a)]. The lattice planes that give rise to diffraction are denoted by solid lines with the corresponding Miller indices.

order peaks of Fig. 2(b) are the (101) reflections, while the second peak may be simultaneously the first order of the (020) reflection. The third-order peak of Fig. 2(b) could not be assigned, but is probably due to the (121) reflection. Because the (110) diffraction occurs in the horizontal plane in the case of  $\omega=(60 \times m)^\circ$ , as seen from

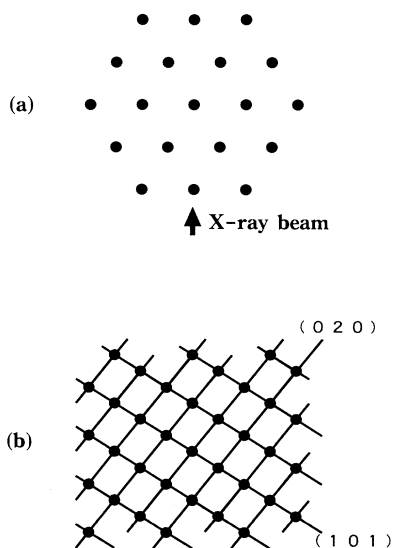


FIG. 4. A schematic illustration of the bcc lattice for  $\omega=30^\circ$  [Fig. 2(b)]. For the legend, see Fig. 3.

Fig. 3, the diffraction angle  $2\theta$  equals  $2\bar{\theta}$ , because  $\cos\phi$  equals unity. Then, using Eq. (1), from the peak positions observed in Fig. 2(a), the distance ( $d_{110}$ ) between the (110) planes was determined to be 2100 Å.

From  $d_{110}$ , the diffraction angles  $2\theta$  from the (101) and (020) planes in Fig. 4 were calculated to be  $(150 \times n)''$  and  $(210 \times n)''$ , respectively. These  $2\theta$  values are consistent with the peak positions observed in Fig. 2(b) because  $2\theta=2\bar{\theta}/\cos\phi$  and the  $\phi$  values are  $54.7^\circ$  and  $35.3^\circ$  for the (101) and (020) planes, respectively. The first order of the (020) reflection is thus at  $2\bar{\theta}=170''$ , while that of the (101) reflection is at  $85''$ . It is recalled that the "infinitely long and thin" beam allowed us to observe the (020) and (101) reflections ( $\phi \neq 0$ ) for the present camera system.

The bcc structure appears to be the only one to explain the observed scattering profiles. We note that the (110) plane is practically parallel to the capillary surface, which is consistent with the experimental results obtained by Sogami and Yoshiyama from Kossel line analysis for polystyrene latex dispersions.<sup>3</sup> Furthermore, the fact that the bcc structure was found in the present work is also in qualitative agreement with their results that the bcc structures are favored for small particles, like the present ones, at low concentrations.

The lattice constant  $a$  obtained by using  $d_{hkl}=a/(h^2+k^2+l^2)^{1/2}$  for cubic lattices with  $d_{110}=2100$  Å was 3000 Å. The closest interparticle distance  $2D_{\text{exp}} [(3^{1/2}/2) \times a]$  was 2600 Å, whereas the average interparticle distance  $2D_0 [(3^{1/2}/2) \times (8\pi/3c)^{1/3} \times R]$  from the particle concentration  $c (=0.0376)$  was 2900 Å for bcc symmetry. It is obvious that  $2D_{\text{exp}}$  is smaller than  $2D_0$ . This inequality relation was first noticed from a single broad x-ray-scattering peak given by polyacrylate solutions<sup>8</sup> and from direct microscopic measurements on latex dispersions.<sup>9</sup> It was inferred to be due to the non-space-filling nature of the ordered structures, in other words, the two-state structure containing localized ordered structures in coexistence with free macroions or particles. With several orders of Bragg diffraction observed in the present case, together with the powder patterns previously observed,<sup>7</sup> we can state that the ambiguity of the previous inference based on the single broad peak or on the microscopic (local) information has been removed,<sup>10</sup> and by simple arithmetic that the crystal occupies  $(2600/2900)^3=0.72$  of the total dispersion volume and the rest (0.28) contains voids and/or free particles for the present case. Clearly contraction takes place in the process of crystallization as was found by us<sup>8,9,12</sup> and others.<sup>13</sup>

It is to be remarked that Sogami and Yoshiyama recently found by the Kossel line analysis for the present dispersion that the lattice structure is bcc and its lattice constant is 3140 Å,<sup>14</sup> in agreement with the present result.

We mention that the Hosemann plot<sup>15</sup> or the application of the Scherrer equation<sup>16</sup> to determine the size of the ordered structure was unsuccessful; the crystal was too large under the present conditions. Finally, it is noted that a single bcc crystal cannot fill up the entire space inside the capillary, because the inner surface of the

capillary has a curvature. In the space between the curved surface and the planar surface of the crystal there must be somehow distorted crystals, small crystals, or free particles.

Sincere thanks are due to Martin V. Smalley, Polymer Phasing Project, ERATO, JRDC, Keihanna Plaza, Kyo-

to 619-02, Japan for discussions and his kind help in preparing the manuscript. Special thanks are due to Dr. J. Yamanaka for his determination of the specific gravity and the charge density of the sample. The authors would like to thank Nippon Shokubai Co., Ltd. for the kind donation of the samples.

---

\*Author to whom correspondence should be addressed.

<sup>1</sup>For a convenient recent review, see, for example, S. Doshō *et al.*, *Langmuir* **9**, 394 (1993).

<sup>2</sup>A. Kose, M. Ozaki, K. Takano, K. Kobayashi, and S. Hachisu, *J. Colloid Interface Sci.* **44**, 330 (1973).

<sup>3</sup>T. Yoshiyama, I. S. Sogami, and N. Ise, *Phys. Rev. Lett.* **53**, 2153 (1984); I. S. Sogami and T. Yoshiyama, *Phase Transitions* **21**, 171 (1990).

<sup>4</sup>H. Matsuoka, K. Kakigami, N. Ise, Y. Kobayashi, Y. Machitani, T. Kikuchi, and T. Kato, *Proc. Nat. Acad. Sci. USA* **88**, 6618 (1991).

<sup>5</sup>U. Bonse and M. Hart, *Z. Phys.* **189**, 151 (1966).

<sup>6</sup>H. Matsuoka, K. Kakigami, and N. Ise, *The Rigaku Journal* **8**, 21 (1991).

<sup>7</sup>H. Matsuoka, K. Kakigami, and N. Ise, *Proc. Jpn. Acad.* **67B**, 170 (1991); H. Matsuoka and N. Ise, *Chemtract* **4**, 59 (1993); H. Matsuoka *et al.*, *J. Phys. (Paris)* **3**, 451 (1993).

<sup>8</sup>N. Ise *et al.*, *J. Am. Chem. Soc.* **102**, 7901 (1980).

<sup>9</sup>N. Ise *et al.*, *J. Chem. Phys.* **78**, 536 (1983).

<sup>10</sup>The Bragg spacing being smaller than the average spacing was reported by Daly and Hasting (Ref. 11) but they attributed this surprising finding to evaporation of the solvent. In the present work, the dispersion capillary was sealed with silicone rubber so that the question of solvent evaporation does not arise.

<sup>11</sup>J. G. Daly and R. Hasting, *J. Phys. Chem.* **85**, 294 (1981).

<sup>12</sup>N. Ise, K. Ito, H. Matsuoka, and H. Yoshida, in *Ordering and Phase Transitions in Colloidal Systems*, edited by A. K. Arora and B. V. R. Tata (VCH Verlag, New York, 1994).

<sup>13</sup>For example, E. A. Kamenetzky, L. G. Magliocco, and H. P. Panzer, *Science* **263**, 207 (1994).

<sup>14</sup>T. Yoshiyama and I. S. Sogami (unpublished).

<sup>15</sup>A. M. Hindleleh and R. Hosemann, *Polymer* **23**, 1101 (1982).

<sup>16</sup>See, for example, B. D. Cullity, *Elements of X-Ray Diffraction* (Addison-Wesley, Reading, MA, 1978), Chap. 3.